

PHASE TRANSFORMATIONS IN TOOL ALLOYS WITH
INTERMETALLIC - CARBIDE HARDENING

I.K. Kupalova, V.A. Landa,*
E.I. Malinkina, and M.N. Fadyushina

UDC 669.15'25'27:621.785.36

Carbon-free and low-carbon cobalt - tungsten alloys are intermediate in strength and red hardness between high-speed steels and metal - ceramic hard alloys [1]. These alloys are easily worked when hot and all types of metal-cutting tools can be produced from them by conventional metallurgical and mechanical techniques.

These alloys are hardened by precipitation of intermetallic or intermetallic and carbide phases. The phase transformations in these alloys differ from those in other tool materials and are of theoretical as well as practical interest (to determine the optimal compositions).

Iron-base NK-1 tool alloys [2] were investigated (0.35% C, 20% W, 20% Co, 4% Cr, 1.5% V, 0.5% Mo, and other elements within the conventional limits for high-speed steels).

Samples 6 × 6 × 60 mm for x-ray structural, electromagnetic, and mechanical analysis and samples 3 mm in diam. and 30 mm long for high-temperature magnetic analysis (anisometric) were obtained by casting, forging, and appropriate thermal and mechanical treatments.

The phase composition of the alloy was determined by x-ray structural analysis in the URS-50I diffractometer, using Co radiation and a scintillation counter.

The x-ray patterns show indices of Fe_α phase, M₆C carbides (base of Fe₃W₃C), and the rhombohedral intermetallic compound Co₇W₆. The patterns show no other phases. When the carbon content of the alloy is reduced the intensity of M₆C lines decreases. Thus, no carbides are observed in the surface decarburized during annealing, but only α phase and a considerable quantity of Co₇W₆.

To determine the relative amounts of intermetallic and carbide phases x-ray patterns were made at reduced contrast in the range of 22°30' - 25°30'. Such patterns showed three lines: 1) (110)_β of Fe_α; 2) (343) of Co₇W₆; 3) [(133) (511)]_α of M₆C.

* Deceased.

TABLE 1

Material	Quench temp., °C	HRC	ρ, μΩ·cm	H _c , Oe	4πI _s , G
Annealed condition					
Alloy	—	40	65	30	16 000
R18	—	18	42	13	16 500
Quenched condition					
Alloy	1280	45	95	103	13 300
Alloy	1350	45	98	112	12 700
R18	1280	62	75	76	12 500

Note: The width of (211) was 7.9 mm for the alloy and 8.8 mm for R18.

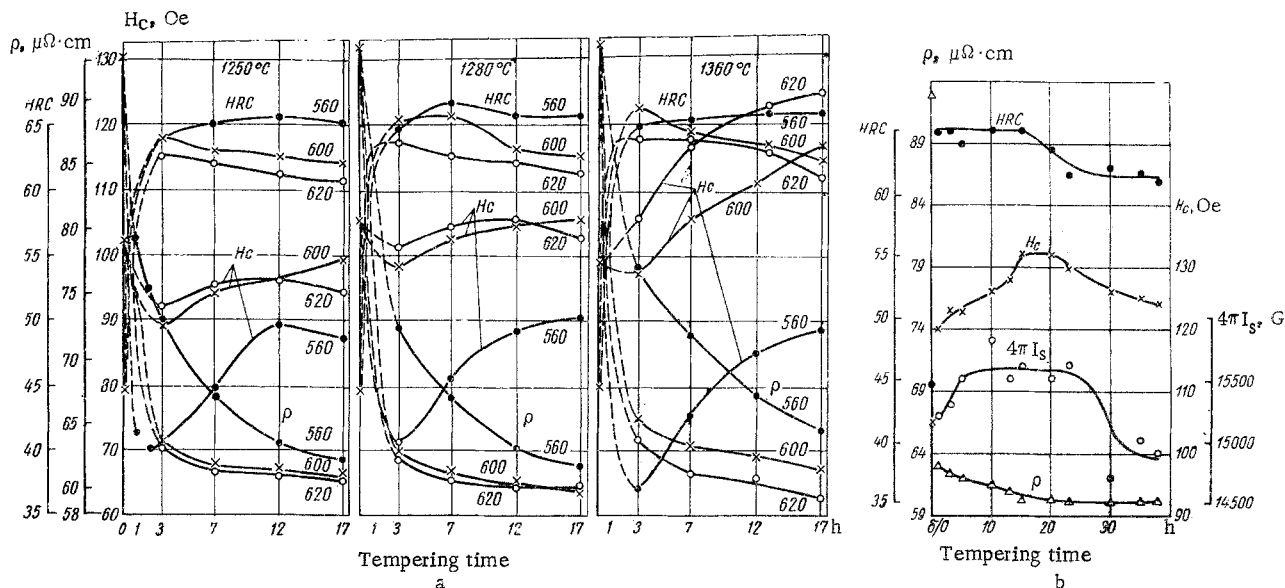


Fig. 1. Variation of the hardness and physical properties of the alloy with the tempering time at different temperatures (a) and at 630°C (b).

Since the lines of the intermetallic and carbide phases are broadened much less than the α phase lines after mechanical and heat treatments, the relative concentrations of ordered phases can be determined from the height of these lines, using the relationship

$$K = (343)_\alpha \text{ Co}_7\text{W}_6 / [(333) (511)]_\alpha \text{ M}_6\text{C}.$$

For the annealed alloy $K = 0.35$.

The value of K changes with the carbon content:

%C	K
0.10	2.2
0.32	0.43
0.35	0.35
0.38	0.177
0.41	0.192

Thus, the value of K depends on the carbon content in alloys of the type investigated (in the annealed condition). From this index one can calculate the degree of decarburation of the surface layers. The properties of the alloys investigated are given in Table 1.

Steel R18 and the alloy contain ferrite and M_6C carbide after annealing and quenching from all temperatures. Apart from these phases, the annealed alloy contains Co_7W_6 and the steel R18 quenched from 1280°C contains austenite.

Under certain annealing conditions no intermetallic phase is observed in the x-ray patterns due to its dispersity.

During quenching of the alloy the Co_7W_6 is completely dissolved at a considerably lower temperature than the M_6C . To determine the solution temperature range of Co_7W_6 during heating to quenching temperature an x-ray phase analysis was made after quenching the alloy from 900–1200°C with holding 2–6 min. On heating up to 1150°C the lines of the intermetallic phase were clearly visible on the x-ray patterns.

On heating at 1150°C and higher only the lines of the Fe_α phase and M_6C carbide remained on the x-ray patterns, i.e., the intermetallic phase passes completely into solution. This was confirmed by the metallographic examination. Residual austenite was completely absent after quenching due to the isothermal and martensitic transformation of the alloy.

From the isothermal transformation diagram of austenite* for austenitizing at 1280°C obtained with the Akulov torque magnetometer it follows that the Curie temperature of the alloys is 900°C (loss of 99% magnetizability), which is 130°C above that of R18 steel. The M_s point is 350°C, which is 150–170°C above that of steel R18. The martensitic transformation concludes at 100°C, i.e., M_f lies above room temperature, which also is responsible for the lack of residual austenite in the alloy after quenching.

By comparison with high-speed steels the region of the upper (pearlitic) transformation in the alloy is 100°C higher and the intermediate (bainitic) transformation of austenite is absent (soaking up to 10 h). The absence of residual austenite after quenching permits single tempering of the alloys, unlike high-speed steels.

The alloys quenched from 1250, 1280, and 1350°C were tempered up to 10 h at 560, 600, and 620°C. At 630°C the tempering time was 40 h. The variation of the hardness and electromagnetic characteristics of the alloy after tempering under some of these conditions is shown in Fig. 1.

The data indicate intensive hardening processes at 560–630°C involving the precipitation of carbide and intermetallic phases. The substantial hardening from HRC 45 to 66 during tempering, the high red hardness Kr_{58} at 720°C, and the satisfactory strength $\sigma_{bend} = 200\text{--}240 \text{ kg/mm}^2$ provide high cutting properties.

The curve of the variation of coercive force with tempering conditions resembles that for the hardness but is shifted toward higher temperatures and longer tempering times, as in the case of high-speed steels.

Since the variations of the hardness and coercive force reflect the different stages of precipitation hardening and weakening during precipitation and coalescence, it must be assumed that the precipitation of the carbide and intermetallic hardening phases develops over a considerable period of time.

The reduction of the specific electrical resistivity during tempering is similar to that in high-speed steels: the higher the quenching temperature and the lower the tempering temperature, the greater the reduction of ρ [3].

The variation of magnetic saturation with tempering time is unusual (Fig. 1b). On tempering 5 h at 630°C the magnetic saturation increases and then remains unchanged up to 23 h. Between 23 and 30 h it decreases again. The specific electrical resistivity remains unchanged at this same time.

This variation of magnetic saturation during tempering may be due to the fact that in the alloys investigated, which contain no residual austenite, the increase of $4\pi I_s$ is due only to impoverishment of the carbon solid solution in alloying elements during tempering. There is a parallel reduction of magnetic saturation due to the increase in the concentration of paramagnetic phases — intermetallic and carbide. These two opposing processes are responsible for the unusual variation of the magnetic saturation.

In high-speed steels the values of $4\pi I_s$ are somewhat higher after high-temperature tempering than after annealing, which is sometimes disregarded in calculating the amount of residual austenite (the so-called negative concentration of residual austenite on high-temperature tempering of high-speed steels).

Analysis of the data obtained indicates that in alloys with several hardening phases the phases dissolved first during heating to quenching temperature are precipitated last during tempering, which determines the temperature range of the hardening, i.e., the red hardness of the alloy. This rule applies to alloys hardened by intermetallic and carbide phases and steels with several carbides that differ in stability, e.g., $M_{23}C_6$, M_6C , and MC .

CONCLUSIONS

1. The iron-base tool alloy (0.3–0.4% C, 20% W, 20% Co, 4% Cr), which is hardened by precipitation of intermetallic and carbide phases, consists of Fe_α phase, M_6C carbide, and the intermetallic compound Co_7W_6 in the annealed condition.
2. The extent of decarburizing can be determined from the relative intensities of the Co_7W_6 and M_6C lines on the x-ray patterns.

* The anisometric investigation was conducted by A. D. Yakovleva.

3. During heating to quenching temperature the Co_7W_6 is dissolved first, and then M_6C . All the Co_7W_6 is dissolved at 1150°C , while part of the M_6C remains in the form of excess carbide even after quenching from 1350°C .

4. The M_s - M_f points of the alloy are 130 - 150°C higher than for high-speed steels of the usual composition and the M_f point is above room temperature, due to which the quenched alloy contains practically no residual austenite.

5. The hardness of the alloy as cast, annealed, and quenched is approximately the same (HRC 40-45).

6. The absence of residual austenite after quenching permits single tempering of the alloy.

7. The alloy is hardened in tempering at 560 - 630°C due to the precipitation of carbide and intermetallic phases. The hardness is increased to HRC 67 at a red hardness of Kr_{58} up to 720°C and strength σ_{bend} up to 240 kg/mm^2 , and the cutting and technological properties are high.

LITERATURE CITED

1. V. A. Brostrem and Yu. A. Geller, Metal, i Term. Obrabotka Metal., No.11 (1966).
2. Tetsu to Hagane, 49, No.3 (1963).
3. L. A. Chudnovskaya and I. K. Kupalova, in: Physical Methods of Studying and Checking the Structure of Tool Steels [in Russian], Mashgiz, Moscow (1963).